

Studies on Si-doped AlGaN Epilayers

Kamran Forghani

Growth optimization of Si doped AlGaN epilayers—with 20 %, 30 % and 45 %Al content—grown on AlGaN-sapphire by MOVPE was investigated. We could realize n-type carrier concentrations from about $2 \times 10^{18} \text{ cm}^{-3}$ to $1 \times 10^{19} \text{ cm}^{-3}$. The layers with high levels of dopants suffer from crack formation. Therefore, we used a short period super lattice to manage the strain between the doped layer and the undoped buffer layer. The XRD investigations were performed to reveal the strain evolution in our layers with respect to the dopant concentration. Using variable temperature Hall measurements on such films, the activation energy of the Si-donors was evaluated. We found a fairly small activation energy confirming that the doping concentrations are in the range of the Mott transition.

1. Introduction

AlGaN as a wide-bandgap semiconductor material has found increasing scientific and practical interest in the last few years. This is, in large part, due to its use in UV light emitting diodes (LEDs) [1] as well as laser diodes (LDs) [2]. Although LEDs and LDs have been commercially developed in the near-UV (above 400 nm) and visible region, the construction of such devices becomes much more challenging as the wavelength shortens. One essential part of UV-LEDs and UV-LDs is the growth of n-doped AlGaN epilayers. It is expected that the realization of a reasonable n-type conductivity in AlGaN is more challenging than in GaN due to the formation of defects with increase of the Al- or Si-content. Additionally, an increase of the donor activation energy with increasing Al-content is expected because of a gradual increase in the effective electron mass and a decrease in the dielectric constant. Therefore, we study the doping of AlGaN with Si as a common donor. The grown Si-doped films must be suitable templates for the growth of LEDs and LDs. Therefore, they must be crack-free. However, the critical thicknesses of the doped films is much less than in the undoped films. We have attempted to find out the possible reasons as this phenomenon is not yet well understood.

Nowadays, there are many reports about the activation energy of Si in n-doped AlGaN (from GaN:Si to AlN:Si). However, these values vary over a wide range as different buffer layers (in terms of crystal quality) and different dopant concentrations were investigated. In order to understand the effect of dopant concentration on activation energy, the films with different doping concentration, but with similar buffer layers are compared in this work.

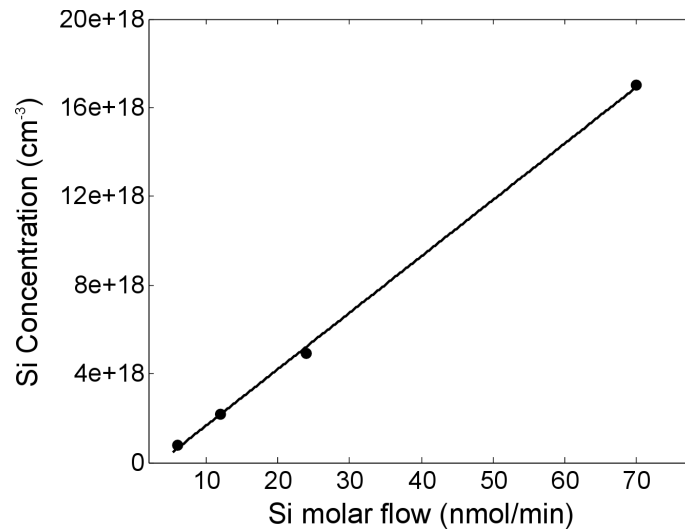


Fig. 1: Linear relation between Si concentration measured by SIMS and Si molar flow in samples A, B, C and D.

2. Experimental Details

All samples investigated in this study were grown on (0001) sapphire substrates in a low-pressure horizontal reactor (Aixtron AIX-200/4 RF-S). Trimethylgallium (TMGa) and trimethylaluminum (TMAI) were used as group-III precursors and ammonia as group-V precursor. The aluminum incorporation in the undoped buffer layers was set to about 20%, 30% and 45% as confirmed by photoluminescence (PL). The standard growth temperature was set to 1120 °C. Similar to our high quality GaN layers [3], we used a nucleation layer (NL) of oxygen doped AlN with a thickness of about 25 nm. Silane was used as the Si source.

Some of the samples which were used for the following investigations were grown on our previously developed AlGaIn epilayers with an in-situ deposited SiN nano-mask [4]. The nano-masking improves the crystal quality [5] of the epilayers leading to higher performance of LEDs grown on such templates [6].

Variable temperature Hall-effect measurements were applied to determine the activation energy of the donors in the AlGaIn films.

3. Results and Discussions

3.1 Effect of Si doping on strain

In order to investigate the effect of Si concentration on the evolution of strain in AlGaIn films, four samples A, B, C, D—all with 20% Al—were grown with identical structures; 500 nm Si-doped AlGaIn on 500 nm undoped AlGaIn. The doping levels in those samples were $8.0 \times 10^{17} \text{ cm}^{-3}$, $2.2 \times 10^{18} \text{ cm}^{-3}$, $4.9 \times 10^{18} \text{ cm}^{-3}$ and $1.7 \times 10^{19} \text{ cm}^{-3}$, respectively for samples A–D. There were no intentional measures taken in order to increase the crystal quality of the epilayers. The Si incorporation into the solid phase (AlGaIn) shows a linear behavior with the Si effective molar flow in this range (Fig. 1).

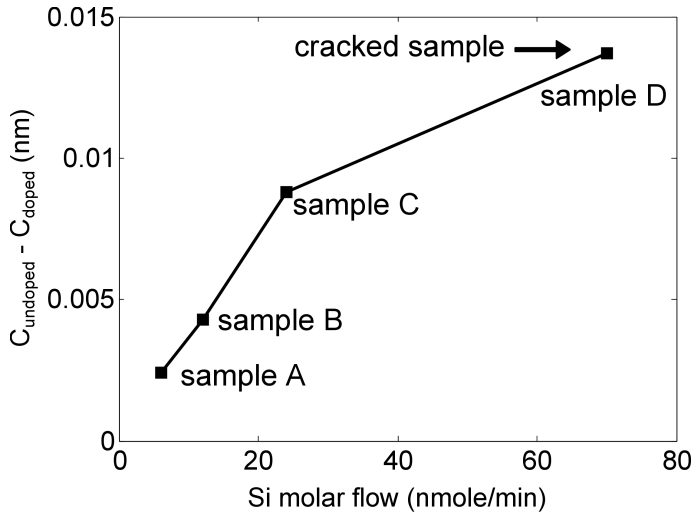


Fig. 2: The mismatch between c-lattice constant of the buffer layer and the doped layer increases as Si concentration increases.

The samples were crack free, except the last sample (sample D) which had a very high doping level. In other words, we observed that, the higher the Si concentration is, AlGa_N epilayers exhibit less critical thicknesses. XRD Ω -2 Θ scans—(004) reflections—of the samples A–D reveal that the c-lattice constant shrinks as the Si concentration increases (Fig. 2).

Reciprocal space mapping (RSM) of asymmetric (105)-reflections was carried out (Fig. 3) in order to determine the strain of these layers.

As the Si concentration increases from sample A to slightly higher concentrations in sample B, a broadening of the XRD peak is visible. Emergence of a side peak with lower q_z and higher q_x in reciprocal space is visible as the Si concentration increases from sample B to samples C and D.

Clearly, the a-lattice constant of the top doped epilayer increases with increasing Si concentration while the c-lattice constant decreases, implicating a biaxial tensile strain induced in the crystal structure by Si doping. This Si induced-tensile strain was observed also by others, e.g. by Romano et al. [7] in GaN. They have concluded that this might be due to a coalescence phenomenon during growth, as a slight roughening of the film surface is often observed in Si doped GaN epilayers. However, our AlGa_N:Si films showed even smoother surfaces with Si doping. According to M. Moram et al. [8] Si is able to 'pin' the dislocations, hindering them from climbing. Preventing the dislocations from climb during film growth leads to less absorption of tensile stress that develops during growth.

However, similar investigation on AlGa_N films seems to be necessary in order to understand whether this argument still holds in the case of Si-doped AlGa_N films.

3.2 Electrical properties of n-doped AlGa_N epilayers

We have grown several samples with Al contents of 20%, 30% and 45% in order to evaluate the possible donors' activation energy of the AlGa_N over the composition range of 20% to 45%. A summary of the structure of the samples is listed in Table 1, and the details can be found in Ref. [9]. Samples B and C as described in section 3.1 consist of

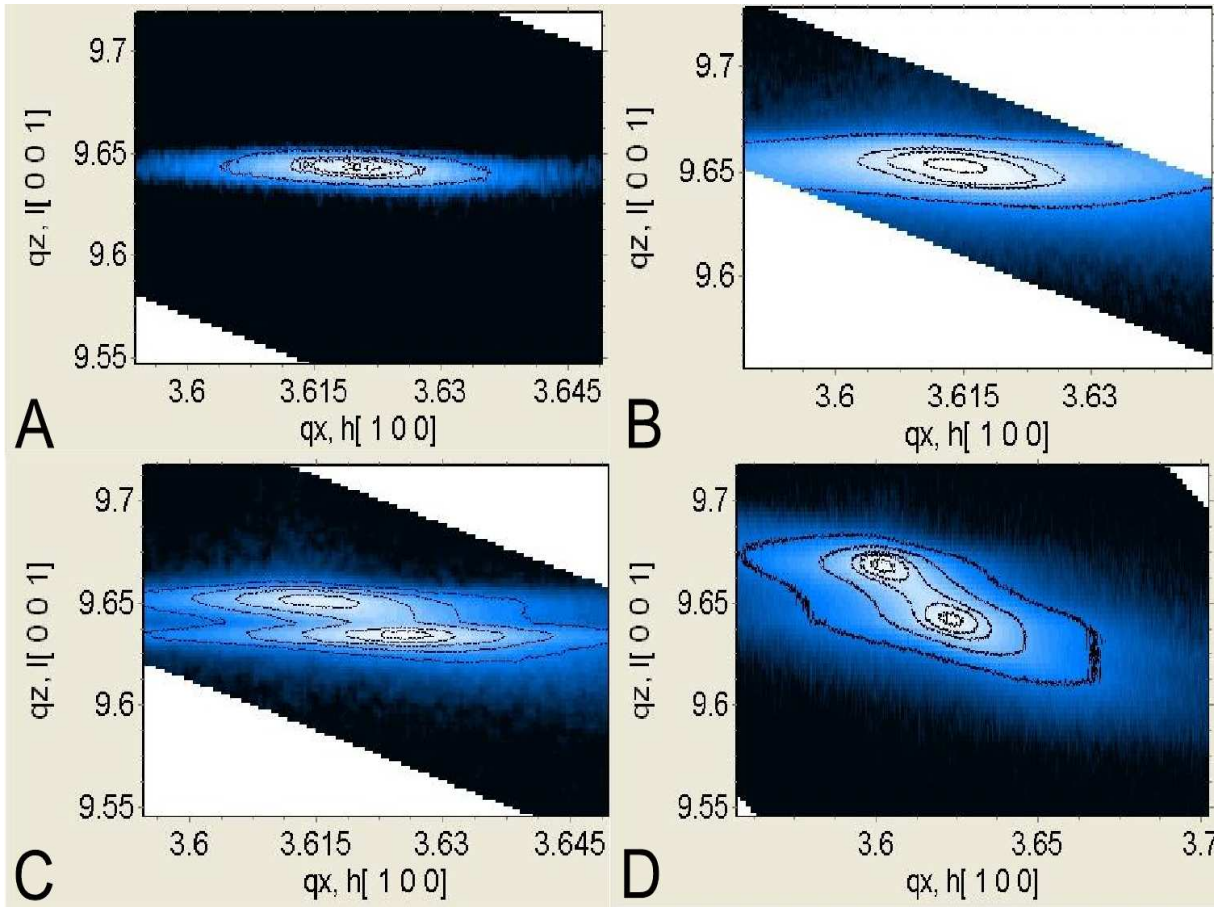


Fig. 3: Reciprocal space mappings of samples A, B, C and D: An increase of the a-lattice constant ($\propto \frac{1}{q_x}$) in comparison to the undoped AlGaIn buffer layer is visible. The opposite scenario is valid for the c-lattice constants ($\propto \frac{1}{q_z}$), confirming the symmetric measurements.

Table 1: Structure and doping doses of the samples shown in Fig. 4.

Sample	Al content	Si-molar flow (nmole/min)	SiN nanomasking	SPSL
B	20 %	12	—	—
C	20 %	24	—	—
E	20 %	12	150 nm above NL	—
F	30 %	12	On NL	—
G	30 %	24	On NL	Yes
I	45 %	12	—	Yes

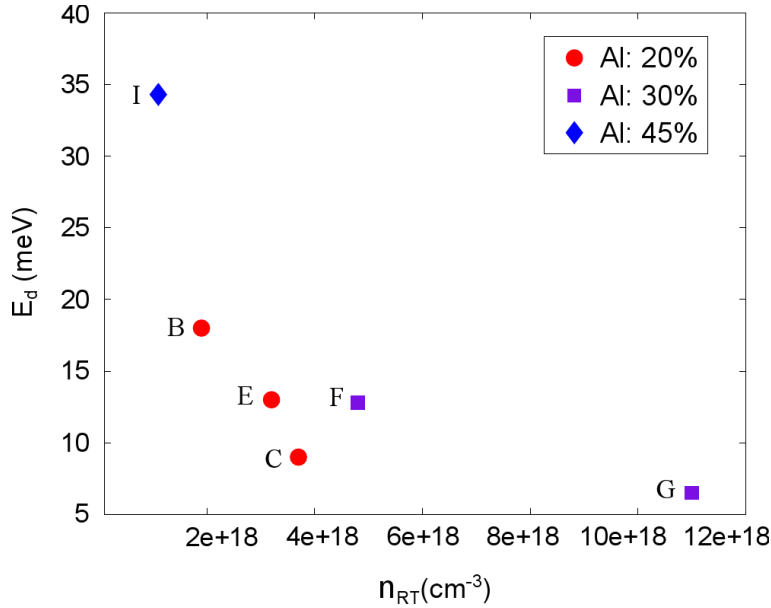


Fig. 4: Activation energy of the Si-donors (ΔE_d) evaluated for several AlGaN epilayers with different Si contents or Al contents; samples' details in Table 1.

500 nm $\text{Al}_{0.2}\text{Ga}_{0.8}\text{N}:\text{Si}$ grown on an undoped $\text{Al}_{0.2}\text{Ga}_{0.8}\text{N}$ buffer layer with the thickness of 500 nm. Therefore, we can compare the change in the activation energy due to the change of the dopant concentration in $\text{Al}_{0.2}\text{Ga}_{0.8}\text{N}$. Sample E was grown on our high quality $\text{Al}_{0.2}\text{Ga}_{0.8}\text{N}$ templates with a 3400 nm thick undoped part and a 500 nm doped part on top. A SiN nanomask was deposited *in-situ* 150 nm above the NL to significantly reduce the dislocation density in this sample. The silane effective molar flow was set identically to that of sample B. Thus, we could study the influence of the SiN nanomask in our templates on the donors' activation energy. In order to have a similar comparison, we have grown samples F and G with higher Al content (30%). These samples are $\text{Al}_{0.3}\text{Ga}_{0.7}\text{N}:\text{Si}$ with different Si doping levels grown on buffer layers with a SiN nanomask deposited on the NL. Because the SiN interlayer is less effective at higher Al contents, we did not use that interlayer for the growth of sample I ($\text{Al}_{0.45}\text{Ga}_{0.55}\text{N}$). It consists of a 500 nm thick un-doped $\text{Al}_{0.45}\text{Ga}_{0.55}\text{N}$ buffer layer with 500 nm thick $\text{Al}_{0.45}\text{Ga}_{0.55}\text{N}:\text{Si}$ on top. The silane molar flow for the growth of the doped part is identical to that of samples B, E and F (Table 1).

As the Al content—or the silane molar flow—increased in the films, severe crack formation was evident. As investigated in section 3.1, this is due to the generation of a tensile strain with increasing Si content in the AlGaN films. In order to suppress the formation of cracks, we have tried to compensate the rising tensile strain by inducing more compressive strain from the buffer layer. Therefore, a series of short period super lattices (SPSLs) were grown below the Si-doped part to reduce the average a-lattice constant of the buffer layer. In the current work, the SPSL consists of 120 pairs of $\text{AlN}(2\text{ nm})\text{—Al}_x\text{Ga}_{1-x}\text{N}(3.5\text{ nm})$ sequences for an $\text{Al}_x\text{Ga}_{1-x}\text{N}$ film. The growth of such SPSLs resulted in the growth of completely crack free wafers and very smooth surfaces. The samples that required the growth of SPSLs are indicated in Table 1 (samples G and I).

The activation energy of the donors (ΔE_d) was evaluated for these layers using variable temperature Hall measurements. The details of these evaluations are explained in Ref. [9].

The donor activation energy is depicted in Fig. 4 for the samples shown in Table. 1 with different Si- and Al-contents.

Looking to samples B and C (similarly samples F and G), it is clear that as the doping concentration is increased ΔE_d approaches very low values (below 10 meV). This dependency of ΔE_d to carrier concentration can be explained by the Mott transition also known as metal-nonmetal transition [10]. For the samples with higher concentrations of Si compared to the Mott critical concentration, one can expect to observe a more metallic behavior of conductivity. A continuous increase of the Si concentration leads to the formation of a donor band. As such an impurity band widens further with an increase of the impurity content, it can even overlap with the conduction band [11]. This delocalization of the carriers leads to a very low activation energy.

The critical Mott density N_c is given by [10, 12]:

$$N_c \approx \left(\frac{0.25}{a_b}\right)^3, \quad (1)$$

where, a_b is the effective Bohr radius. Our calculations show that N_c is equal to $1.1 \times 10^{18} \text{ cm}^{-3}$ for GaN, $2.0 \times 10^{18} \text{ cm}^{-3}$ for $\text{Al}_{0.20}\text{Ga}_{0.80}\text{N}$, $2.6 \times 10^{18} \text{ cm}^{-3}$ for $\text{Al}_{0.30}\text{Ga}_{0.70}\text{N}$ and $3.7 \times 10^{18} \text{ cm}^{-3}$ for $\text{Al}_{0.45}\text{Ga}_{0.55}\text{N}$. The calculated value for N_c of GaN in Ref. [12], based on Mott's model, confirms the correctness of our calculations.

All samples depicted in Fig. 4 except sample I ($\text{Al}_{0.45}\text{Ga}_{0.55}\text{N}$) have donor concentrations fairly higher than N_c . Looking to sample E in Fig. 4, it is clear that this sample has higher carrier concentration than sample B while both have been grown with the same silane molar flow. A similar situation exists for samples F and G which have been doped with silane molar flows, identical to samples B and C respectively. A possible explanation might be the deposition of a SiN interlayer during growth of such films which increases the total Si content of the films. SiN deposition may increase the Si impurity during the growth or enhance the Si diffusion to the upper layers.

Comparing samples C (20 %) and F (30 %) which show similar carrier concentrations, one can conclude that the sample with higher Al content has higher activation energy (Fig. 4). A similar comparison can be made between sample B (with 20 % Al content) and sample I (with 45 % Al-content).

4. Conclusion

Growth of n-doped AlGa_N with 20 %, 30 %, 45 % Al-content was realized. As the Al-content in the epilayers or the dopant concentration increases, cracks were observed on the surfaces. XRD investigations showed that the crack formation is due to the increase of the tensile strain in the doped part of the films due to the Si doping. However, the mechanisms contributing to the rising tensile strain is not yet clear. A series of SPSLs was grown in order to compensate the tensile strain by inducing more compressive strain.

We have calculated critical donors concentration (Mott density) for our AlGa_N:Si films. Having evaluated all the samples with variable temperature Hall-effect measurements, we

confirmed for the samples with Si concentrations higher than N_c , the donors activation energies are very low. In such samples, donor activation energy decreases with increasing Si content. It was found that samples with higher Al-content exhibit also higher donor activation energies. The samples with a SiN nanomask show much higher carrier concentrations than the samples without any SiN nanomask. This might be due to Si diffusion during growth originated from deposition of the SiN interlayers.

5. Acknowledgments

The assistance of M. Gharavipour in characterization of the samples and respective evaluations is gratefully acknowledged. The author would like to thank R. Rösch and I. Argut for preparing samples for Hall measurements and K. Thonke and F. Lipski for fruitful discussions, B. Neuschl for providing PL evaluations in addition to the Fraunhofer Institute for Applied Solid State Physics for providing SIMS evaluations. The author acknowledges the support from Dr. W. Limmer for Hall-effect measurements. This work was financially supported by the German Federal Ministry of Education and Research (BMBF) within the framework of the “Deep UV-LED” project.

References

- [1] A. Khan, K. Balakrishnan, and T. Katona, “Ultraviolet light-emitting diodes based on group three nitrides”, *Nat. Photonics*, vol. 2, pp. 77–84, 2008.
- [2] H. Yoshida, Y. Yamashita, M. Kuwabara, and H. Kan, “A 342-nm ultraviolet AlGa_N multiple-quantum-well laser diode”, *Nat. Photonics*, vol. 2, pp. 551–554, 2008.
- [3] J. Hertkorn, P. Brückner, S.B. Thapa, T. Wunderer, F. Scholz, M. Feneberg, K. Thonke, R. Sauer, M. Beer, and J. Zweck, “Optimization of nucleation and buffer layer growth for improved GaN quality”, *J. Cryst. Growth*, vol. 308, pp. 30–36, 2007.
- [4] J. Hertkorn, F. Lipski, P. Brückner, T. Wunderer, S.B. Thapa, F. Scholz, A. Chuvilin, U. Kaiser, M. Beer, and J. Zweck, “Process optimization for the effective reduction of threading dislocations in MOVPE grown GaN using in situ deposited SiN_x masks”, *J. Cryst. Growth*, vol. 310, pp. 4867–4870, 2008.
- [5] K. Forghani, M. Klein, F. Lipski, S. Schwaiger, J. Hertkorn, R.A.R. Leute, F. Scholz, M. Feneberg, B. Neuschl, K. Thonke, O. Klein, U. Kaiser, R. Gutt, and T. Passow, “High quality AlGa_N epilayers grown on sapphire using SiN interlayers”, *J. Cryst. Growth*, vol. 315, pp. 216–219, 2011.
- [6] M. Kunzer, R. Gutt, L. Kirste, T. Passow, K. Forghani, F. Scholz, K. Köhler, and J. Wagner, “Improved quantum efficiency of 350 nm LEDs grown on low dislocation density AlGa_N buffer layers”, *Phys. Stat. Sol.* (accepted, to be published in 2011).

- [7] L.T. Romano, C.G. Van de Walle, J.W. Ager, W. Götz, and R.S. Kern, “Effect of Si doping on strain, cracking, and microstructure in GaN thin films grown by metalorganic chemical vapor deposition”, *J. Appl. Phys.*, vol. 87, pp. 7745–7783, 2000.
- [8] M.A. Moram, M.J. Kappers, F. Massabuau, R.A. Oliver, and C.J. Humphreys, “The effects of Si doping on dislocation movement and tensile stress in GaN”, (to be published in *J. Appl. Phys.*)
- [9] M. Gharavipour, *Doping studies of AlGaN with high Al content*, Master Thesis, Ulm University, Ulm, Germany, Jan. 2011.
- [10] N.F. Mott, “Metal-insulator transition”, *Rev. Mod. Phys.*, vol. 40, pp. 677–683, 1968.
- [11] H. Morkoç, *Handbook of Nitride Semiconductors and Devices, Electronic and Optical Processes in Nitrides* (1st ed.), pp. 589–590, Berlin: Wiley-VCH, 2008.
- [12] A. Ferreira da Silva and C. Persson, “Critical concentration for the doping-induced metal-nonmetal transition in cubic and hexagonal GaN”, *J. Appl. Phys.*, vol. 92, pp. 2550–2555, 2002.